Tin Oxide Films Made by Physical Vapor Deposition-Thermal Oxidation and Spray Pyrolysis

Sang Hyun Park,[†] Young Chan Son,[†] William S. Willis,[‡] Steven L. Suib,*[,†,‡,§] and Kenneth E. Creasy*[,∥]

Department of Chemistry, Box U-60, Institute of Materials Science, and Department of Chemical Engineering, University of Connecticut, Storrs, Connecticut 06269-4060, and Olin Chemicals, Olin Corporation, 350 Knotter Drive, POB 586, Cheshire, Connecticut 06410-0586

Received October 14, 1997. Revised Manuscript Received June 15, 1998

Tin oxide films have been prepared by physical vapor deposition of Sn followed by thermal oxidation and by spray pyrolysis of $SnCl_4$ or $SnCl_4 \cdot 5H_4O$ mixed with CH_3OH. Phase changes and surface morphologies during the syntheses were monitored by X-ray diffraction and scanning electron microscopy. Electrical resistance and UV−visible transmittance of tin oxide films prepared by both methods were measured. The peak shapes of the Auger Sn $M_4N_{45}N_{45}$ transition of the prepared tin oxide films were compared to those of commercial SnO and SnO_2 and used to determine rough values of the oxidation state of Sn. Oxygen/tin ratios in the films were determined from analyses of scanning Auger microprobe and X-ray photoelectron spectroscopy and are all less than 2. Auger depth profiles with thermally oxidized tin oxide films on glass substrates show an overlapping region between the tin oxide film and the substrate. These films were tested as sensors for CH_2Cl_2 in O_2. The mixed phase ($SnO \cdot SnO_2$) tin oxide films prepared by temperature-programmed thermal oxidation of Sn showed better sensing behavior to CH_2Cl_2 than single phase (SnO or SnO_2) films.

I. Introduction

Tin oxide materials are used in a variety of applications as antistatic films, thin film resistors, and antireflecting coatings in solar cells. Tin oxides have also been investigated as gas sensors for H_2, O_2, CO, CO_2, NO_x, H_2S, CH_4, C_2H_5OH, and C_6H_6.[1−4] High electrical conductivity, good chemical stability, high transparency (compared to other metal oxides) in the visible region, and strong physical and chemical interactions with adsorbed species are some properties of SnO_2. SnO_2 is also stable thermally in air at up to 500 °C and mechanically in aqueous media. SnO_2 thin films can be made easily by standard thin film technologies, which means low cost of production, high reliability, and good reproducibility. By sol−gel methods, catalysts or doping materials can be added easily to SnO_2 to increase sensitivity and selectivity for certain gases. However, surface morphology, chemical composition, defects of the tin oxide material, optical properties, and electrical behavior need to be controlled and understood before SnO_2 can be used as gas sensors.

Several methods such as spray pyrolysis,[5,6] sol−gel dip coating,[7] chemical vapor deposition (CVD),[8] and physical vapor deposition (PVD)[9,10] have been used to control or change the properties of tin oxide films. Spray pyrolysis and PVD thermal oxidation have been used here. Spray pyrolysis is simple and inexpensive and allows for the preparation of large films compared to other methods.[5,6,11] PVD thermal oxidation methods lead to roughened surfaces and mixed phases of tin oxide films depending on the conditions of thermal oxidation. Tin oxide films prepared by PVD have large contact areas (due to surface roughening), mixed valent tin, defects, and higher light absorption than stoichiometric SnO_2. The PVD films are also free of organic materials from precursors and have less chance of being contaminated during preparation than films prepared by other methods.

Previous research of films prepared by PVD thermal oxidation for gas sensing have focused on preparation temperatures of 500 °C with formation of 15 000 Å thick films.[12] However, the reported procedure only showed data for the films prepared at 500 °C with 15 000 Å Sn

* To whom correspondence should be addressed.
[†] Department of Chemistry, University of Connecticut.
[‡] Institute of Materials Science, University of Connecticut.
[§] Department of Chemical Engineering, University of Connecticut.
[∥] Olin Corp.

(1) Schierbaum, K. D.; Weimar, U.; Gopel, W. *Sens. Actuators B* **1990**, *2*, 71−78.
(2) Principi, G.; Maddalena, A.; Gupta, A. *Hyperfine Interactions* **1991**, *69*, 619−622.
(3) Omar, O. A.; Ragaie, H. F.; Fikry, W. F. *J. Mater. Sci. Mater. Electronics* **1990**, *1*, 79−83.
(4) Vasu, V.; Subrahmaanyam, A. *Thin Solid Films* **1991**, *202*, 283−288.
(5) Acosta, D. R.; Maldonado, A.; Asomoza, R. *J. Mater. Sci. Mater. Electronics* **1993**, *4*, 187−191.
(6) Miki-Yoshida, M.; Andrade E. *Thin Solid Films* **1993**, *224*, 87−96.
(7) Maddalena, A.; DAl MAschio, R.; Dire, S.; Raccanelli, A. *J. Non-Crystalline Solids* **1990**, *121*, 365−369.
(8) Oyabu, T. *Appl. Phys.* **1982**, *53*, 2785−2787.
(9) Kulkarni, A. K.; Knickerbocker, S. A. *Thin Solid Films* **1992**, *220*, 321−326.
(10) Lalauze, R.; Pijolat, C. *Sens. Actuators* **1984**, *8*, 227−233.
(11) Miki-Yoshida, M.; Andrade, E. *Thin Solid Films* **1993**, *224*, 87−96.

S0897-4756(97)00672-8 CCC: $15.00
Published on Web 08/22/1998

thick films.[12] Sintering can occur during thermal oxidation[13] on Si substrates. The resultant films were used to sense hydrocarbons.[13]

Different characterization techniques have been used to understand the physical and chemical properties of tin oxide materials.[9,14−18] For the determination of tin oxide composition, X-ray diffraction (XRD) has been commonly used. However, XRD patterns can often be misleading because they show bulk crystalline phases, not those on the surface. Amorphous phases cannot be detected by XRD. X-ray photoelectron spectroscopy (XPS) and Auger electron spectroscopy (AES) have been used to determine the composition of the surface of SnO_x films. Recent AES and XPS results indicate that the relative peak intensity of the Sn $M_4N_{45}N_{45}$ to O $KL_{23}L_{23}$[19,20] transitions and Sn $3d^5/_2$ binding energies are not reliable for SnO_x oxidation state determination.[14,15] There are differences in peak intensities and positions of the Sn $M_4N_{45}N_{45}$ Auger transition due to oxidation states of tin oxide materials.[16−18]

The goal of our research is to make tin oxide thin films and to control properties such as crystallinity, surface morphology, chemical composition, optical properties, and electrical behavior. Tin oxide films have been prepared by PVD of tin, followed by thermal oxidation, and by spray pyrolysis of $SnCl_4 \cdot 5H_2O$ mixed with methanol, or $SnCl_4$. Films were characterized by XRD with energy-dispersive X-ray analysis (EDX), XPS, scanning Auger microprobe (SAM), UV−visible spectroscopy, and resistance measurements. A two-probe electrical resistance method was used on the tin oxide films. Such films have been used to sense CH_2Cl_2 in O_2.

II. Experimental Section

A. Preparation of Tin Oxide Films by Spray Pyrolysis. $SnCl_4$ was prepared with 7 g of $KMnO_4$ (EM Science, Cherry Hill, NJ), 250 mL of concentrated HCl (J. T. Baker, Phillipsburg, NJ), and Sn metal (99.99%, Alfa Co., Danvers, MA).[21] H_2O was added to $SnCl_4$ to make $SnCl_4 \cdot 5H_2O$. Solutions for spray coating were prepared by mixing 25 g of $SnCl_4 \cdot 5H_2O$ with 6 mL of methanol in a beaker. After positioning substrates on a firebrick wrapped with aluminum foil, the substrates were covered with Al foil again to prevent rapid temperature decrease upon removal and placed in a furnace at 500 °C. After 10 min of heating, the substrates were removed and immediately sprayed with the $SnCl_4 \cdot 5H_2O$/methanol solution using O_2 as carrier gas. Further heating of the spray-coated films[3,7,11,22] at 500 °C for 1 h was sometimes needed to burn out residual hydrocarbons from the spray solution.

B. Preparation of Tin Oxide Films by PVD and Subsequent Thermal Oxidation. Sn metal films were prepared by thermal heating of Sn metal under high vacuum in the 10^{-7} Torr range. Sn metal chunks were mounted on a specimen holder (RDM5−18389, R. D. Mathis, Long Beach, CA) in a Denton vacuum coater (DV-502A, Denton Vacuum, Inc., Morristown, NJ). The glass slide substrates (1 × 1 × 3 mm, Fisher Scientific) or quartz slides (1 in. × 1 in., Quartz Scientific, Inc., Fairport Harbor, OH) were cleaned in soapy water, followed by immersion in KOH−ethanol solution and in dilute HCl solution for several hours, and finally washed with doubly distilled water. The thickness of the Sn films during deposition was monitored with a quartz crystal thickness monitor (TM-100, Maxtex, Inc., Torrance, CA). After Sn metal films were prepared, they were transferred to a furnace at constant temperatures of 210, 400, and 500 °C and at temperature ramps from 200 to 500 °C for 14 h after preheating at 200 °C for 10 h. All thermally oxidized samples were stored in a desiccator containing anhydrous $CaCl_2$ and P_2O_5.

C. X-ray Diffraction. A Scintag XDS-2000 X-ray diffractometer with Cu Kα radiation was used for measurement of sample crystallinity. Diffraction patterns were collected at a step size of 0.05° 2θ with fixed Cu Kα radiation, and the background was subtracted by a linear interpolation method. The most intense peak of each pattern was assigned an intensity of 100 cps.

D. Scanning Electron Microscopy (SEM) and Energy Dispersive X-ray Analysis. An Amray model 1810D SEM with an Amray model PV 9800 EDX system was used to determine surface morphologies of the films and their compositions semiquantitatively up to 1 μm in depth. Thermally oxidized and spray-coated samples were cut into 1 cm × 1 cm pieces and mounted on sample holders with carbon paste.

E. X-ray Photoelectron Spectroscopy. A Leybold Heraeus LHS-10 spectrometer with an EA 10 hemispherical analyzer detector and an Al Kα X-ray radiation (1486.6 eV) source was used for analysis of Sn and O content in tin oxide films up to 50 Å. The Au $4f^7/_2$ transition was used for calibration of the instrument. Step sizes of 1 eV for survey spectra and 0.1 eV with pass energies of 50 eV for detailed spectra were used.

F. Scanning Auger Microprobe. A Perkin-Elmer PHI model 610 scanning Auger microprobe equipped with a cylindrical mirror analyzer was used for surface compositional analysis of the films within 50 Å. A 3 keV electron beam and 30 nA sample current were used with a tilt angle of 30°. Depth profiles of a thermally oxidized films were done to determine compositional changes through the film using Ar ion sputtering with a sample current of 0.5 μA, an electron beam voltage of 3 keV, and a sputter size of 2 mm × 2 mm. Pressure during the analyses was maintained in the 1 × 10^{-10} Torr range.

G. UV−Visible Spectrometer and Resistance Measurements. A Hewlett-Packard diode array spectrophotometer 8452A with a deuterium lamp and a 2 mm × 18 mm diode array containing 328 individual photodiodes was used for absorbance measurements of spray-coated and PVD-coated films during thermal oxidation. Samples were fixed in the sample compartment with tape. A quartz slide was used for background subtraction. Electrical resistance measurements were obtained with a 7551 digital multimeter (OMEGA, Stamford, CT) in air at room temperature, using the two-probe method. Resistance measurements were repeated five times for sample sizes of 1 in. × 1 in.

H. Sensor Experiments. Tin oxide films were cut into 1 in. × 0.2 in. pieces. Each end of the film was tightly wrapped with two pure gold foils, secured with 18 K gold clips, and connected to the multimeter through two pure gold wires for resistance measurements. The films were placed in a custom-designed test chamber made of Pyrex glass, where temperature under controlled atmosphere can be varied. Resistance changes of the films with 100, 1000, and 5000 ppm CH_2Cl_2 in O_2 were measured with a two-probe method at 300 °C. Flow rates of 113 mL/min were used for sensing CH_2Cl_2. Resistance curves

(12) Yoo, K. S.; Cho, N. W.; Song, H. S.; Jung, H. J. *Sensors Actuators* **1995**, *B, 24−25*, 474−477.
(13) Chung. W. Y.; Kim, T. H.; Hong, Y. H.; Lee, D. D. *Sensors Actuators* 1995, *B, 24−25*, 482−485.
(14) Themlin, J. M.; Chtaib, M.; Henrard, L.; Lambin, P.; Darville, J.; Gilles, J. M. *Phys. Rev. B* **1992**, *46*, 4, 2460−2466.
(15) Jie, L.; Chao, X. *J. Non-Crystalline Solids* **1990**, *119*, 37−40.
(16) Suib, S. L.; Stucky, G. D.; Blattner, R.; Weller, P. F. *J. Solid State Chem.* **1980**, *31*, 387−392.
(17) Hoflund, G. B. *J. Chem. Mater.* **1994**, *6*, 562−568.
(18) Drawdy, J. E.; Hoflund, G. B.; Davidson, M. R.; Upchurch, B. T.; Schryer, D. R. *Surf. Interface Anal.* **1992**, *19*, 559−564.
(19) Kim, K. H.; Park, C. G. *J. Electrochem. Soc.* **1991**, *138*, 2408−2412.
(20) de Fresart, E.; Darville, J.; Gilles, J. M. *Solid State Commun.* **1980**, *37*, 13−17.
(21) Sperry, E. A. *J. Soc. Chem. Ind.* **1908**, *27*, 312−314.
(22) Segal, S. R.; Park, S. H.; Suib, S. L. *J. Chem. Mater.* **1997**, *9*, 98−104.

Table 1. Summary of Experimental Conditions for Tin Oxide Thin Films by Thermal Oxidation and Spray Pyrolysis

entry	starting material	oxidation condition	crystalline phases
S1	1000 Å Sn on glass	210 °C after 120 h	SnO
S2	1000 Å Sn on glass	400 °C after 40 h	SnO
S3	1000 Å Sn on glass	500 °C, 0.5 h	$SnO{\cdot}SnO_2$
S4		1 h	SnO_2
S5		1.5 h	SnO_2
S6		5 h	SnO_2
S7		18 h	SnO_2
S8	1000 Å Sn on glass[a]	300 °C, 5 h	SnO
S9		450 °C, 10 h	$SnO{\cdot}Sn_3O_4$
S10		480 °C, 12 h	$SnO{\cdot}SnO_2$
S11		500 °C, 22 h	$SnO{\cdot}SnO_2$
S12		500 °C, 32 h	$SnO{\cdot}SnO_2$
S13	$SnCl_4{\cdot}5H_2O$ mixed with CH_3OH	spray on 500 °C substrate	SnO_2

[a] After preheating at 200 °C for 10 h.

of the prepared films were obtained from room temperature to 400 °C for a 4 h period in O_2.

III. Results

Starting materials, oxidation conditions, and crystalline phases as determined by X-ray diffraction (see section III A) are given in Table 1. Samples are identified as **S*X***, ***X*** = 1−13, for different preparations.

A. X-ray Diffraction and Scanning Electron Microscopy. Tin oxide films oxidized at temperatures above 520 °C with tin films on glass substrates appeared less conductive than films oxidized at lower temperatures. Direct heating above the melting point of Sn (231.9 °C)[23] led to sintering of tin films. On the basis of two factors, thermal oxidations were carried out at different temperatures and led to different tin oxide phases. Two approaches were used, one with constant temperatures of 210 and 500 °C and another with programmed temperatures from 200 to 500 °C after preheating at 200 °C for 10 h.

Sn films of 1000 Å thickness on glass were heated at a constant temperature of 210 °C. XRD measurements were taken after 18, 31, 54, and 120 h (**S1**). Regardless of oxidation time, all samples showed similar XRD patterns with four peaks at *d* spacings of 4.85, 2.99, 2.69, and 2.42 Å due to SnO (Figure 1A, JCPDS no. 6-395). There were no significant changes in the intensity, position, and width of the peaks during heating. The color of all films turned from shiny metallic to dark gray in the first 15 h of thermal oxidation and remained dark gray as shown in Figure 2. Colors of the films during oxidation at 500 °C change from light gray (after 0.5 h) to semitransparent (after 12 h). There is a visual color change from dark gray to semitransparent with temperature increase from 200 to 500 °C. There was loss of Sn of about 50% (by an ICP-AA method) after thermal oxidation at 500 °C. These color changes are possibly due to further oxidation of SnO (JCPDS no. 6-395, black) to SnO_2 (JCPDS no. 41-1445, white), loss of Sn, and film sintering when treatment temperatures are increased.

(23) CRC handbook, 75th ed; CRC: Boca Raton, FL, 1995.

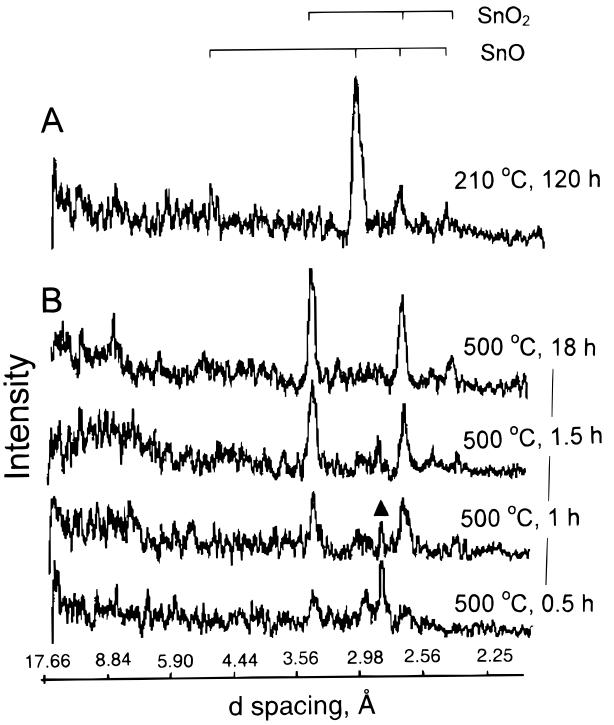

Figure 1. XRD patterns of the thermally oxidized tin oxide films at constant temperature: (A) 210 °C with 1000 Å Sn on glass after 120 h (**S1**) and (B) 500 °C with 1000 Å Sn on glass after (1) 0.5 h (**S3**), (2) 1 h (**S4**), (3) 1.5 h (**S5**), and (4) 18 h (**S7**). SnO, JCPDS no. 6-395; SnO_2, JCPDS no. 41-1445; and □, not assigned.

XRD patterns of thermally oxidized 1000 Å Sn films at 500 °C are shown in Figure 1B-1 (after 0.5 h, **S3**), 1B-2 (1 h, **S4**), 1B-3 (1.5 h, **S5**), and 1B-4 (18 h, **S7**). After 0.5 h, three weak broad peaks at 3.35, 2.99, and 2.69 Å as well as a relatively sharp peak at 2.84 (▲) were observed as shown in Figure 1B-1. The peak at 3.35 is attributed to SnO_2, and those at 2.99 and 2.67 are attributed to SnO. The peak at 2.84 is not identified. The intensities of two peaks at 3.35 and 2.64 Å due to SnO_2 (JCPDS no. 41-1445) increase with duration of thermal oxidation (from Figure 1B-1 to 1B-4). Another peak attributed to SnO_2 appeared at 2.37 Å after 18 h (Figure 1B-4). However, the other two peaks at 2.99 and 2.84 Å disappeared after 1.5 h (Figure 1B-3).

SEM photos of the tin oxide film (**S3**, Figure 3A) show that the surface is not uniform, with some particles 1−2 μm in diameter and other particles of 5−6 μm in diameter. EDX results showed that the large particles consist of 96% Sn and 4% Si, while the smaller particles (1−2 μm) are 10% Sn, 82% Si, 2% Na, and 6% Ca. Samples that have been thermally oxidized for longer times (up to 5 h) show more particles of 5−6 μm in diameter (Figure 3B). These particles consist of 76% Sn and 24% Si with 1−2 μm particles consisting of 11% Sn, 83% Si, and 6% Ca.

Thermal oxidation by ramping the temperature from 200 to 500 °C after preheating the samples at 200 °C for 10 h was done with 1000 Å Sn films on glass substrates. Preheating at 200 °C was done to reduce film sintering during thermal oxidation. Figure 4A shows the XRD pattern of a sample (**S8**) taken at 300 °C after 5 h. Two peaks at 4.85 and 2.99 Å due to SnO (JCPDS no. 6-395) are observed. Figure 4B shows an

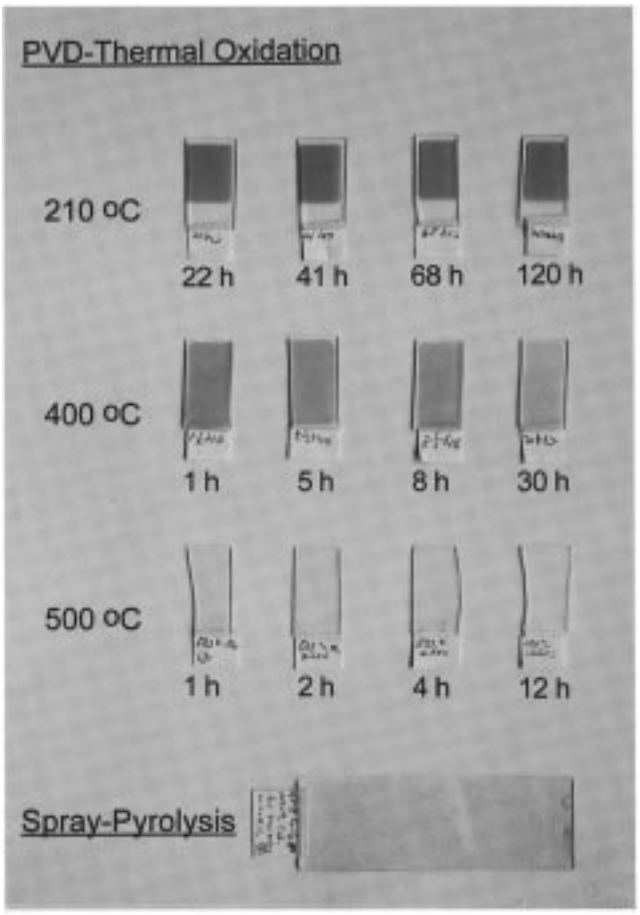

Figure 2. Photographs of tin oxide films prepared by PVD thermal oxidation at different temperatures and by spray pyrolysis.

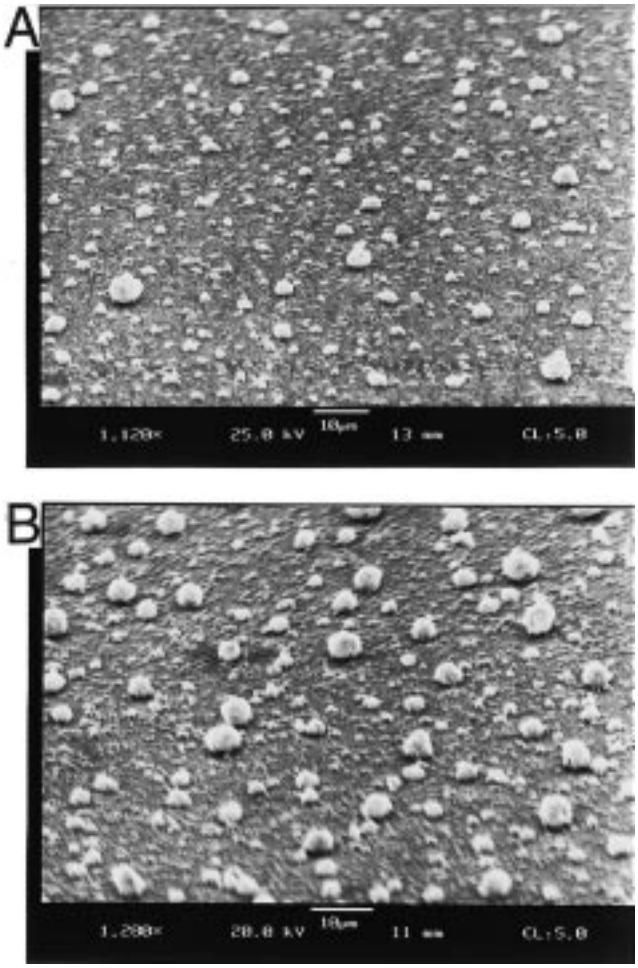

Figure 3. SEM pictures of the tin oxide films (A) **S3** and (B) **S6**.

XRD pattern of a sample (**S9**) taken at 450 °C after 10 h. Several broad peaks at 4.85, 2.99, 2.84, and 2.72 Å as well as two sharp peaks at 2.98 (□) and 2.86 Å (●) are observed. As before, the peaks at 4.85 and 2.99 Å are attributed to SnO. Upon increasing the temperature from 480 °C (Figure 4C with **S10**) to 500 °C (Figure 4D with **S11** and Figure 3E with **S12**), the peaks at 2.99 Å become smaller, but the intensities of the other three peaks at 3.35, 2.64, and 2.37 Å due to SnO_2 are enhanced.

Figure 5A shows the surface morphology of sample (**S10**) heated at 480 °C. Particles on the order of 1−2 μm with no significant sintering are observed. EDX showed that the particles consist of 16% Sn, 78% Si, and 6% Ca. The surface morphology of the sample (**S11**) heated at 500 °C is shown in Figure 5B with particles of various diameters ranging from 1 to 4 μm. The composition of the area with 1−2 μm particles in Figure 5B by EDX is 9% Sn, 83% Si, and 8% Ca. The composition of 4 μm particles is 95% Sn, 3% Si, and 2% Ca.

The XRD pattern of a tin oxide film (**S13**) on glass prepared by spray pyrolysis with $SnCl_4 \cdot 5H_2O$ mixed with CH_3OH is shown in Figure 6A. One small weak peak at 3.35 Å, perhaps due to SnO_2, is observed. Figure 6B shows the surface morphology of the same sample (**S13**). Small cracks are seen at the surface. The composition is 21% Sn, 72% Si, 6% Ca, and <1% Cl, as detected by EDX. The EDX probes a volume that is shaped like a tear drop and has dimensions of about 2 μm depth. The detection of Si by EDX is expected for films that are <2 μm thick.

B. Sheet Resistances during Thermal Oxidation. Sheet resistances of tin oxide films during thermal oxidation of Sn metal films on glass substrates at different temperatures were monitored as shown in Figure 7A,B. Oxidation conditions (200 °C for 10 h, 200−500 °C) used for Figure 4 were applied to 1000 Å Sn films on glass to observe changes in sheet resistance of tin oxide films during oxidation (Figure 7A). Sheet resistances of tin oxide films decreased from 10^7 to 10^4 Ω as the temperature increased from 200 to 500 °C. However, the decrease in sheet resistance is not significant until the temperature reaches 330 °C. A dramatic resistance drop is seen as the temperature is increased above 330 °C. During thermal oxidation at 500 °C, there is a relatively slow decrease in sheet resistance, followed by a gradual increase in resistance.

Sheet resistance measurements were also obtained at a constant temperature of 500 °C with 1000 Å Sn films on quartz (Figure 7B-1) and on glass substrates (Figure 7B-2). Film resistances for the films on quartz are in the range of 10^4−10^5 Ω. There is a small decrease in sheet resistance in the first 2 h of heating followed by a slow increase. A big drop in sheet resistance from 10^6 to 10^4 Ω in the first 2 h of heating is observed for films on glass followed by a big increase to 10^6 Ω upon further oxidation. Samples of 900 Å Sn films on glass were treated at 400 °C (Figure 7B-3). Generally, film resis-

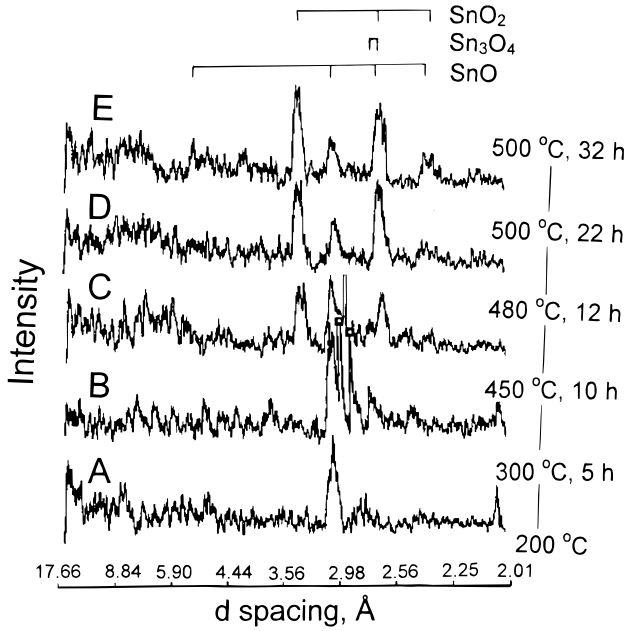

Figure 4. XRD patterns of tin oxide films during temperature-programmed thermal oxidation from 200 to 500 °C after preheating at 200 °C for 10 h: (A) 300 °C after 5 h (**S6**), (B) 450 °C after 5 h (**S9**), (C) 480 °C after 12 h (**S10**), (D) 500 °C after 24 h (**S11**), and (E) 500 °C after 34 h (**S12**). The sample nomenclature and description are given in Table 1; SnO, JCPDS no. 6-395; Sn_3O_4, JCPDS no. 20-1293; SnO_2, JCPDS no. 41-1445; and □, not assigned.

tances are in the range of 10^6 Ω. There is a decrease in film resistance with further heating at 400 °C. Thermally oxidized tin oxide films at 210 °C showed sheet resistances in the range of 10−30 MΩ and no change in resistance during oxidation. Sheet resistances of the spray-coated films are in the range of 10^4−10^6 Ω.

C. Scanning Auger Microprobe. Auger Sn $M_4N_{45}N_{45}$ (423−438 eV in kinetic energy) and O $KL_{23}L_{23}$ (509−511 eV) transitions of tin and tin oxide materials are compared in Figure 8. Before thermal oxidation, the Sn $M_4N_{45}N_{45}$ transitions appear at 430 and 438 eV for 850 Å Sn films on glass after 5 min of sputtering (Figure 8A). However, for commercial SnO (Figure 8E), SnO_2 (Figure 8F) and for tin oxide films prepared by spray pyrolysis (**S13**, Figure 8D) and by thermal oxidation at a constant temperature of 500 °C (**S3**, Figure 8B) and by ramped temperature methods (**S9**, Figure 8C), the transitions of Sn $M_4N_{45}N_{45}$ appear at 423 and 430 eV. The Sn peak at 430 eV (on the low kinetic energy side) has a distinctively higher intensity than the one at 438 eV before oxidation (Figure 8A). The Sn peaks on the low kinetic energy side for heated samples and the SnO_x standards are smaller than the peaks at 430 eV (Figure 8B-F). Relative intensities of oxygen to the first peak of Sn $M_4N_{45}N_{45}$ at low kinetic energy become larger with thermal oxidation (Figure 8A−C). In terms of the peak shapes and intensities of Sn $M_4N_{45}N_{45}$ and O $KL_{23}L_{23}$, the sample treated at constant temperature (500 °C) for 30 min (**S3**, Figure 8B) looks similar to SnO (Figure 8E) and the temperature-programmed sample (**S11**, Figure 8C) is similar to SnO_2 (Figure 8F). The O $KL_{23}L_{23}$ peaks appear at 509 ±1 eV in all samples. The relative intensity ratios of O to the first Sn peak on the lower kinetic energy side (509 eV/423 eV in Figure 8B−F) are different in the various samples. This will be described in detail in the Discussion section.

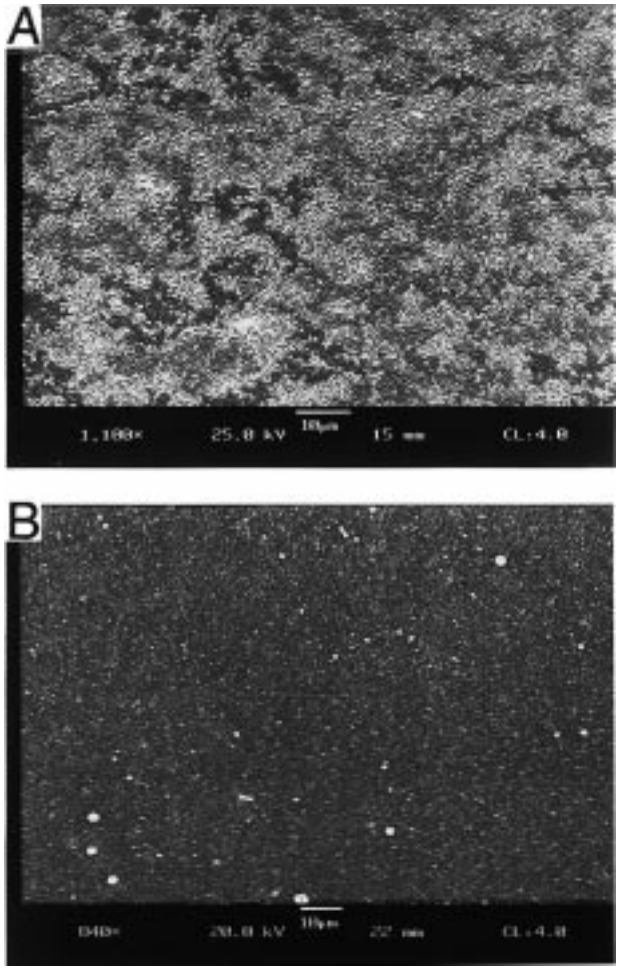

Figure 5. SEM pictures of the tin oxide films (A) **S10** and (B) **S11**.

Chemical composition through the thickness of a tin oxide film prepared by thermal oxidation of 850 Å Sn film on glass at 500 °C for 3 h was examined by Auger depth profiles with Ar ion sputtering. As shown in Figure 9, the amount of Sn appears to be constant up to a certain depth that is equivalent to 8 min of sputtering and decreases gradually after that. Si, believed to be from the glass substrate, increases with sputtering time. The oxygen concentration seems to decrease slightly up to a depth of 8 min of sputtering and increases after that, at which time the Sn content starts to decrease and Si content increases. Adventitious carbon is observed on the surface.

D. Optical Properties. Optical properties of thermally oxidized films (Figure 10A,B-1) and a spray-coated film (Figure 10B-2) were measured. Thermal oxidation of 850 Å Sn on a quartz substrate was done at a programming ramp of 200−500 °C/18 h after preheating at 200 °C for 10 h. Transmittance data for the films taken at 200 °C (Figure 10A-1), 400 °C (Figure 10A-2), 470 °C (Figure 10A-3), and 500 °C after 1 h (Figure 10A-4), 3 h (Figure 10A-5), and 4 h (Figure 10A-6) are displayed. There is an increase in transmittance by tin oxide films as the temperature increases. Higher transmittance in the visible range is observed than in the UV range. Maximum light transmittance in the UV−visible range is over 80%. Figure 10B compares

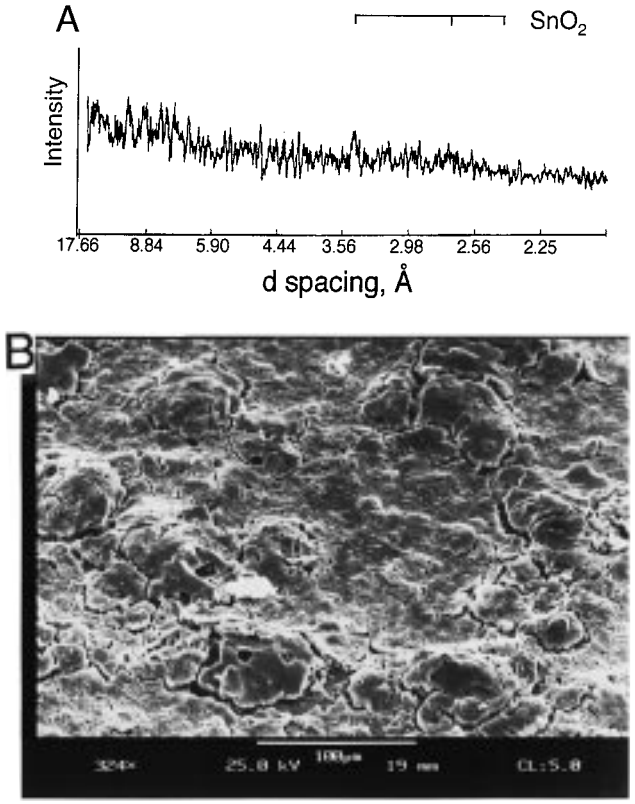

Figure 6. XRD pattern (A) and SEM picture (B) of the spray-coated film (**S13**) on glass with $SnCl_4 \cdot 5H_2O$ mixed with CH_3OH.

the transmittance of two tin oxide films, a spray-coated film of $SnCl_4$ on a quartz substrate heated at 500 °C (Figure 10B-1) and a thermally oxidized film (Figure 10B-2) prepared by PVD followed by thermal oxidation (ramp to 500 °C, 4 h dwell). The spray-coated film shows higher transmittance than the thermally oxidized film.

E. Resistance Characteristic Curve and CH_2Cl_2 Sensing. Resistance characteristic curves (resistance vs temperature) of the tin oxide films under O_2 were monitored as shown in Figure 11. With the temperature increase, there is a gradual decrease followed by a sharp increase in sheet resistance with films prepared by temperature programming (**S11**, Figure 11A), by constant temperature at 500 °C for 5 h (Figure 11B), and by spray pyrolysis (**S13**, Figure 11C). However, a tin oxide film (**S2**, Figure 11D) oxidized at 400 °C shows a relatively rapid decrease and a slow increase. **S11** (Figure 11A), **S2** (Figure 11D), and the film oxidized at 500 °C for 5 h (Figure 11B) show minimum points near 230 °C. The spray-coated film (**S13**) shows higher minima near 280 °C than the other films.

The films were tested for the detection of 100, 1000, and 5000 ppm CH_2Cl_2 in O_2, as illustrated in Figure 12. A thermally oxidized film (**S2**) did not show good sensing behavior as shown in Figure 12A. A 500 °C oxidized film (**S6**) showed a sensing behavior to 100 and 1000 ppm CH_2Cl_2. However, resistance changes are not related to the concentrations of CH_2Cl_2 (Figure 12B). The films prepared by temperature-programmed oxidation (**S11**) and spray pyrolysis (**S13**) showed good sensing behavior. The test results for gas sensing by

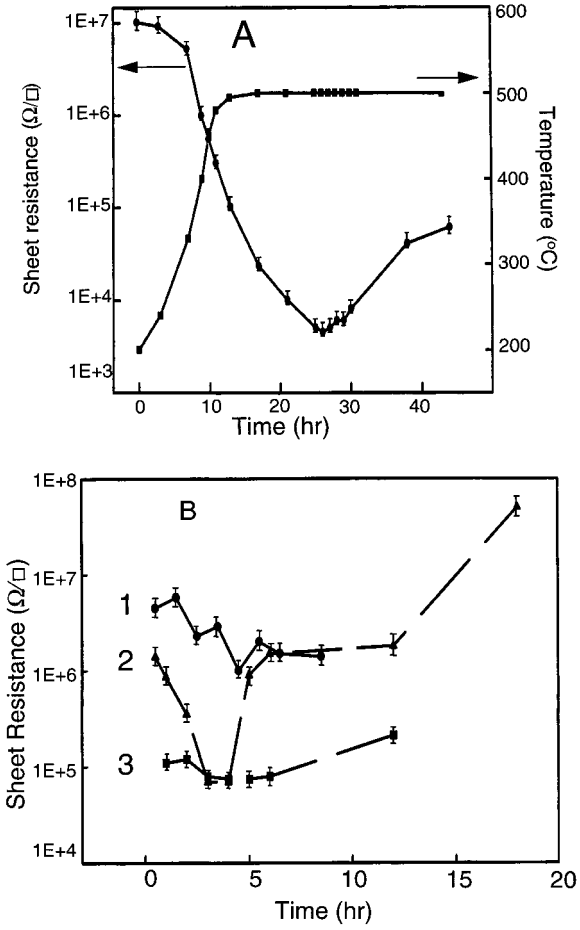

Figure 7. Sheet resistance changes of tin oxide films during thermal oxidation: (A) by temperature programming from 200 to 500 °C (after preheating at 200 °C for 10 h) with 1000 Å Sn film on glass and (B) at constant temperature, (1) at 500 °C with 1000 Å Sn on quartz, (2) at 500 °C with 1000 Å on glass, and (3) at 400 °C with 900 Å Sn on glass.

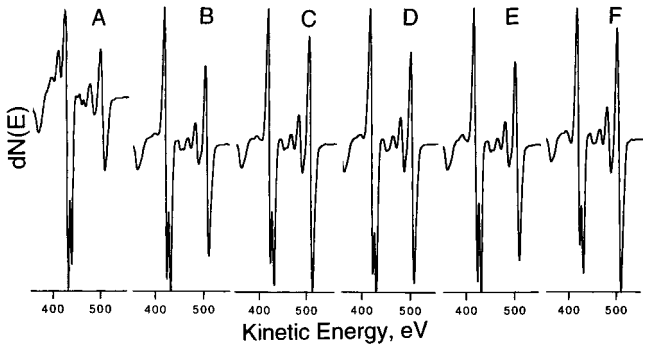

Figure 8. SAM spectra of tin oxide films and commercial SnO and SnO_2 in Sn $M_4N_{45}N_{45}$ and O $KL_{23}L_{23}$ regions: (A) 850 Å Sn film on glass after 5 min sputtering, (B) **S3**, (C) **S11**, (D) **S13**, (E) commercial SnO, and (F) commercial SnO_2.

S11 to 100, 1000, and 5000 ppm CH_2Cl_2 are shown in Figure 12C. The resistance changes are reproducible and are related to the concentrations of CH_2Cl_2.

IV. Discussion

A. Structure and Surface Morphology. Thermal oxidation of tin on glass at 210 °C gives SnO (JCPDS no. 6-395, romarchite) with the maximum peak at 2.99 Å belonging to the (101) reflection. There is no indica-

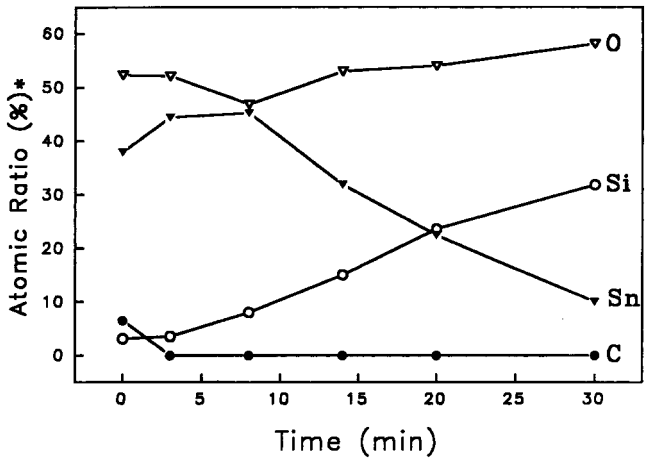

Figure 9. Auger depth profile of the tin oxide film thermally oxidized at 500 °C for 3 h with 850 Å Sn film on glass at 3 keV beam voltage and 0.5 μA sample current. Atomic ratios are calculated on the basis of experimentally determined sensitivity factors.

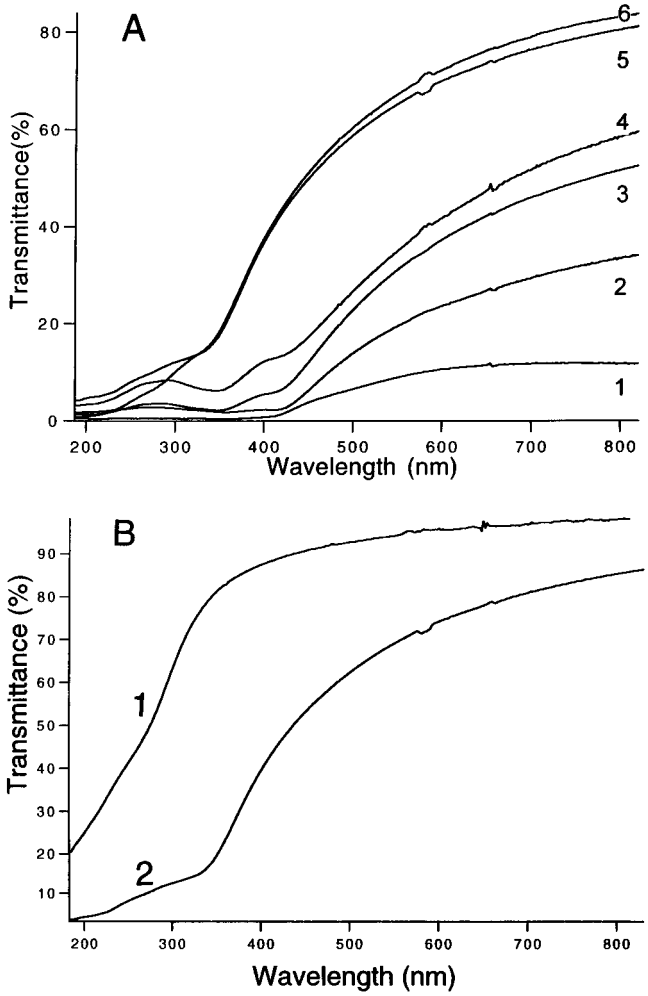

Figure 10. Transmittance comparison of the tin oxide films (A) during temperature-programmed thermal oxidation (200−500 °C) of 850 Å Sn film on quartz at (1) 200 °C, (2) 400 °C, (3) 470 °C, (4) 500 °C after 1 h, (5) 500 °C after 3 h, and (6) 500 °C after 4 h and (B) prepared by two different methods (1) by spray pyrolysis of $SnCl_4$ and (2) by temperature-programmed thermal oxidation (Figure 10A-6).

tion of a further phase change with continued heating at this temperature. There are no XRD peaks observed

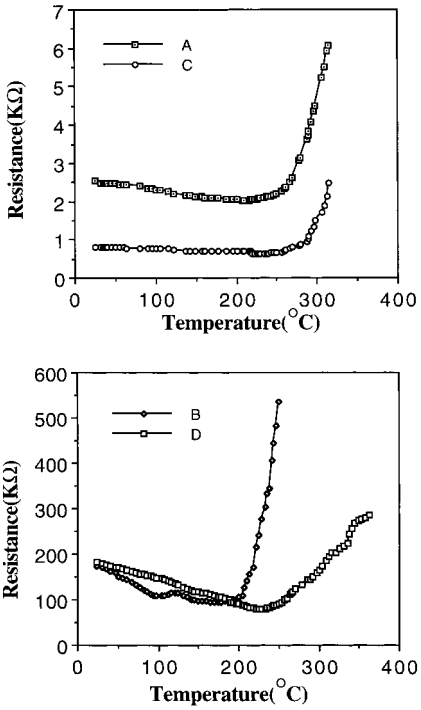

Figure 11. Resistance vs temperature of tin oxide films under O_2 with (A) **S11**, (B) **S6**, (C) **S13**, and (D) **S2**.

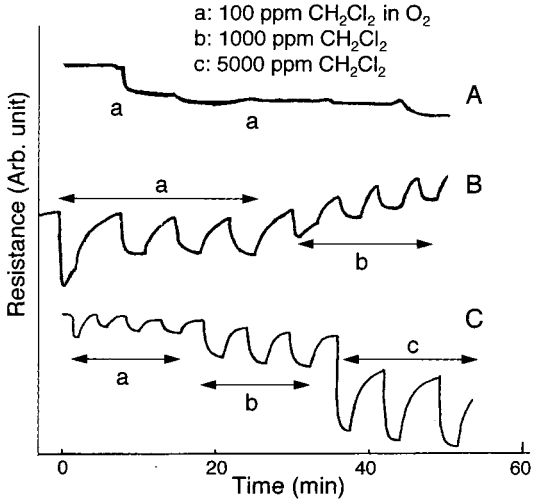

Figure 12. Detection of 100, 1000, and 5000 ppm CH_2Cl_2 in O_2 by tin oxide films (A) **S2**, (B) **S6**, and (C) **S11**.

for SiO_2 or any other Si material. This indicates that no crystalline silicon species are present in these films.

Thermal oxidation at 500 °C (Figure 1B) shows phase changes to SnO_2 via SnO. After 30 min at 500 °C (**S3**), there are some mixed tin oxides, SnO of romarchite and SnO_2 of cassiterite (JCPDS no. 41-1445), as shown in Figure 1B-1. These mixed tin oxides turn into SnO_2, whose peaks appear at 3.35, due to the (110) reflection, 2.64, and 2.37 Å upon further oxidation for 18 h (**S7**, Figure 1B-4). There is another peak at 2.84 Å which diminishes as oxidation continues. Even though the most intense peak matches that of SnO_2 (JCPDS no. 33-1374), an unambiguous assignment cannot be made. The SEM micrograph (**S6**, Figure 3B) shows more particles of 5−6 μm in diameter and fewer small particles between big particles than that of **S3** (Figure 3A). SEM data presented in Figure 3A,B suggest that

there is significant sintering of tin oxides with longer thermal oxidation. More sintering in Figure 3B than in Figure 3A could explain the intensity increase of the SnO_2 peaks from Figure 1B-1 to B-4.

The films (**S8**-**S12**) prepared by temperature-programmed thermal oxidation show different phase changes, as seen in Figure 4. At 300 °C, the major phase identified from XRD is SnO (Figure 4A), believed to be due to the preheating oxidation at 200 °C. After increasing the temperature to 450 °C (**S9**, Figure 4B), several peaks appear near 2.72 Å, due to Sn_3O_4 (JCPDS no. 20-1293). The assignments of the two peaks at 2.98 (□) and 2.86 Å (□) are uncertain. From Figure 4B−E, the three broad peaks due to SnO_2 near 3.35, 2.64, and 2.37 Å have grown and the peak due to SnO (2.99 Å) has decreased. From XRD results, these films are mainly composed of SnO_2 and SnO.

The surface of a film heated at 480 °C (**S10**, Figure 5A) looks smooth, with particles up to 2 μm in diameter. Similarly, less sintering is observed with temperature-programmed oxidation than with constant temperature oxidation at 500 °C (compare Figure 5, parts A and B, with Figure 3, parts A and B). Preheating at 200 °C is believed to stabilize these tin oxide films, which plays an important role in film morphology. Spray-coated samples (**S13**) of $SnCl_4 \cdot 5H_2O$ mixed with CH_3OH also show the SnO_2 phase as shown in Figure 6. In contrast to thermally oxidized samples, the surface of the sample (**S13**) shows no particles on a micron scale, but some cracks, which is apparently different from thermally oxidized samples.

Many crystalline tin oxide films can be made by thermal oxidation of Sn films under different temperature conditions. Previous research has shown that the temperature of the PVD thermal oxidation and spray pyrolysis processes for tin oxidation can influence the crystallinity of resultant metal oxides.[3,7,11,13,24] Less sintering observed for tin oxide films prepared by temperature-programmed thermal oxidation than by constant temperature heating at 500 °C in our research is different from previous research.[13] This may be due a combination of factors, such as different substrates, differences in thickness of Sn films, and different temperature treatments.

B. Chemical Composition. From EDX results with tin oxide films oxidized at different temperature conditions, the particles with 5−6 μm have higher Sn content (over 90% in Sn) than 1−2 μm particles (less than 10%). Spray-coated films have a homogeneous composition with 21% Sn and 72% Si. Impurities of Ca, Na, and Si detected by EDX are believed to be from the glass substrate.

No Si was detected by XPS in the samples except for sample **S7**. Significant sintering due to thermal oxidation over long times (18 h) at 500 °C may explain this observation. However, some Si (<5%) on the surface of the samples only heated at 500 °C (constant temperature) is detected by Auger analyses. This difference in [Si] by the two techniques can be explained by different detection mechanisms. SAM involves analysis of a spot smaller than 2 μm. Samples were mounted with a tilt angle of 30°, which creates a different depth sensitivity and escape depths of Auger electrons as compared to XPS. This signal is likely due to the glass substrate and may indicate holes due to sintering, inhomogeneous coating, or loss of Sn during heating. Note that Si was only detected in the SAM experiments when high temperatures (500 °C) were used. Both SnO and SnO_2 have high melting points and are difficult to vaporize. Perhaps hydrated or hydroxylated tin oxide species were volatilized at 500 °C.

Table 2. O/Sn Ratios at Various Tin and Tin Oxide Films on Glass by XPS and SAM

oxidation time[a]	XPS	SAM	temp (°C)
0[a]	1.0	0.9	room temp
3 min[b]	1.7	nd	500
7 min[b]	1.6	nd	500
1 h[b]	1.9	nd	500
6 h[b]	1.9	1.9	500
18 h[c]	1.6	1.6	200
a few seconds [d]	1.5	1.5	500

Sn = 1000 Å for *a*−*c*; *a*, without sputtering; *b* and *c*, thermal oxidation; *d*, spray coating; nd, no data.

The O/Sn ratios determined by XPS and Auger are compared in Table 2. The ratios measured by both techniques appear to be close. A dramatic increase in the ratio appeared after the first few minutes of heating at 500 °C. O/Sn ratios of the films after 1 and 6 h at 500 °C are the same. Tin oxidation within the analysis depth (up to 50 Å) of XPS at that temperature is complete in less than 1 h and takes place to lower depths of the films with longer heating (in combination with XRD data, Figure 1B). However, the O/Sn ratio did not increase much after 18 h of heating at 200 °C. Oxygen detected from Sn films may be due to adsorbed moisture introduced during sample preparation and tin oxide formed on the surface at room temperature. From Table 2, temperature effects on tin oxidation are more significant than time of oxidation. These data suggest that there is an initial surface oxidation of tin and that buried nonoxidized tin further oxidizes rapidly after 0−3 min heating at 500 °C.

It may be possible to observe more changes in oxidation as a function of thermal heating by Auger methods[16−18] than by XPS. The intensity of the O $KL_{23}L_{23}$ transition at 510 eV in Figure 8C (with **S11**, by temperature-programmed oxidation) is higher than that in Figure 8B (with **S3**, by constant temperature oxidation) and similar to that in SnO_2 (Figure 8F). The similarity between Figure 8B,E and between Figure 8C,E is believed to be due to the oxidation state of Sn in the films. The thermally oxidized films (**S11**) treated for long times contain more oxygen and shows a similar peak shape to that of commercial SnO_2 in the Sn and O transitions. The oxygen peak of Figure 8A after 5 min of sputtering may be due to substrate exposure.

The peak intensity ratio of oxygen to metal in a standard compound (for example, SnO_2) can be used to calculate the atomic ratios of an unknown material.[25] Equation 1 was used to determine atomic ratios as shown below:

$$(N_o/N_m)_{unknown} = (I_o/I_m)_{unknown}(I_m/I_o)_{std}(N_o/N_m)_{std} \quad (1)$$

(24) Vasu, V.; Subrahmanyam, A. *Thin Solid Films* **1990**, *193/194*, 973−980.

(25) Lin, A. W. C.; Armstrong, N. R.; Kuwana, T. *Anal. Chem.* **1977**, *49*, 8, 1228−1235.

Table 3. O/Sn Ratios[a] of Tin Oxide Films on Glass Compared to Commercial SnO and SnO_2

sample	**S3**	**S11**	**S13**	SnO	SnO_2
O/Sn	1.33	1.83	1.73	1	2

[a] According to the eq 1 based on SnO_2 standard.

where N is the atomic number of an element in a formula of the unknown (or standard) and I is the peak intensity (maximum − minimum) of an element after differentiation of raw Auger data. The subscripts, o, m, std, and unknown, stand for oxygen, metal, standard, and unknown compounds.

O/Sn ratios of tin oxide films (**S3**, **S11**, and **S13**) and commercial SnO and SnO_2 are in Table 3. The films formed at different conditions show different O/Sn ratios and less oxygen content than SnO_2. Net oxidation states of Sn in tin oxide films are less than 4+, but higher than 2+, which is also consistent with XRD studies. The films (**S11**) prepared by temperature-programmed oxidation are more oxygen rich than the spray-pyrolyzed film (**S13**). The peak shape of the Sn $M_4N_{45}N_{45}$ transition and the O/Sn ratios obtained from SAM studies may give an indication of oxygen content and net oxidation state of tin within the analysis depth of tin oxide films.

Ar ion sputtering was used to determine the chemical composition and interfacial properties of a thermally oxidized film on a glass substrate. The surface is more Sn rich than the interior. There does not appear to be a distinctive interface between the tin oxide layer and the substrate. The mixed region could suggest that either Si, Sn, or both migrated to the other layers. However, the appearance of Si on the surface is more likely due to sintering and aggregation of tin oxide during oxidation, which exposes the substrate. A small decrease in oxygen content up to 8 min of sputtering could be related to the difficulty of getting oxygen to diffuse inside these films during thermal oxidation. A gradual increase with further sputtering may be due to the SiO_2 substrate. Carbon detected on the surface before sputtering is gone after sputtering and may be due to adsorption of hydrocarbon gases from air onto the surface, a phenomenon previously observed in SnO_2 gas sensors.[25]

C. Overview of Thermally Oxidized Film Structure. The tin oxide films prepared by PVD−thermal oxidation consist of three layers, a top SnO_x layer, a bottom SiO_2 substrate, and an interface containing SnO_x and SiO_2 between the two outer layers. There is no distinct interface between the SnO_x layer and the SiO_2 substrate. Crystallinity of the top SnO_x layer ranges from SnO to SnO_2 with the amount of SnO depending on thermal oxidation conditions. The colors of the films are also dependent upon oxidation conditions as shown in Figure 2, from dark brown (210 °C oxidation) to white (500 °C oxidation) to semitransparent (temperature programmed oxidation and spray pyrolysis). O/Sn ratios of the top SnO_x layers are less than 2, which suggests that the net oxidation state of Sn in the SnO_x layer is lower than 4+.

D. Sheet Resistance and Optical Properties. As reported elsewhere,[5,26] sheet resistances of tin oxide films are affected by the thermal treatment of Sn films. The sheet resistances of the samples treated by temperature programming (Figure 7A) decrease by 3 orders of magnitude when the temperature increases from 200 to 500 °C. Phase changes from SnO (romarchite) to SnO_2 (cassiterite) as detected by XRD are shown in Figure 4. These phase changes may be responsible for the decrease in resistance during the temperature increase. Note that no peaks in the XRD data are observed for Sn metal. Sheet resistances generally decrease at short time followed by an increase with longer thermal oxidation at 500 °C, as shown in Figure 7B-1,2. The small change in Figure 7B-1 (quartz substrate) and the large change of resistance in Figure 7B-2 (glass substrate) may be due to substrate hardness and film sintering, which makes tin oxide films less uniform and causes aggregation of tin oxides. From Figures 3A,B, 5A,B, 7A,B-2, it is believed that preheating produces more stable films and reduces film sintering during thermal oxidation.

A gradual decrease in the sheet resistance in the case of annealing at 400 °C can be explained by slow thermal oxidation of Sn. Spray-coated films on glass and quartz substrates show no significant differences in sheet resistance. Sheet resistances of spray-coated films are believed to be dependent upon temperature of the substrates during spraying. Spray-coated films with $SnCl_4$ or $SnCl_4 \cdot 5H_2O$ mixed with methanol have sheet resistances (4−7 kΩ) as low as those of tin oxide films prepared by temperature-programmed oxidation (Figure 7A).

The transmittance increase shown in Figure 10A with temperature increase is seen in both the UV and visible ranges. This can be attributed to phase changes of tin oxides, from SnO to SnO_2 through Sn_3O_4, as shown in Figure 4. Higher light transmittance is observed with spray-coated tin oxide films than with thermally oxidized films over the whole UV−visible range (Figure 10B). This may be due to the smoother surface of the spray-coated films. Low transmittance with thermally oxidized films may also be due to high absorption by tin oxides other than SnO_2 or by mixed tin oxide phases. The high absorption of thermally oxidized films is expected to lead to enhanced photoeffects with respect to spray-coated films.

E. Resistance Profile and Test of CH_2Cl_2 Sensing Ability. Similar trends of resistance were observed with SnO_2 materials containing some dopants.[27] Our films show slightly higher temperature minima of resistance (230−280 °C) than in previous research (200−230 °C).[28] The reason for this phenomenon is uncertain. However, it may be related to impurities in the films as shown from Auger depth profiles or grain boundary effects, which can cause thermal expansion of tin oxide grains during temperature increase.

The tin oxide films prepared by temperature-programmed oxidation and by spray pyrolysis showed good sensing behavior with CH_2Cl_2. **S11** containing SnO and SnO_2 phases showed good sensing behavior. Irregular sensing responses with films oxidized at 400 and 500

(26) Janata, J. In *Principles of Chemical Sensors*; Plenum Press: New York, 1989, Chapter 4.

(27) Gordillo, G.; Moreno, L. C.; de la Cruz, W.; Teheran, P. *Thin Solid Films* **1994**, *252*, 61−66.

(28) Cheong, H. H.; Choi, J. J.; Kim, H. P.; Kim, J. M.; Churn, G. S. *Sensors Actuators* 1992, B, 227−231.

°C were observed. Each of the films oxidized at 400 and 500 °C consist of mainly single phases of SnO or SnO_2. Even though there are significant differences in the mechanism of film sintering with respect to previous researc,[13] the mixed tin oxide phase films show better sensing behavior than single-phase tin oxide films as previously suggested. Crystallinity of the tin oxide films is believed to play a more important role than surface morphology in gas sensing. A detailed description of the detection of chlorinated methanes with these films will appear elsewhere.[29] Preliminary results suggest that resistance decreases with hydrogen/halogen carbon complexes (such as CH_2Cl_2, shown here, and for $CHCl_3$) but increase when hydrogen is not present (CCl_4).

V. Conclusions

Thermal oxidation of Sn films can give different phases of tin oxides on the basis of oxidation conditions. SnO (romarchite) can be made by thermal oxidation at 210 °C and SnO_2 (cassiterite) by thermal oxidation at 500 °C via SnO. Thermal oxidation via programmed temperature, 200−500 °C after preheating at 200 °C, gives many tin oxide phases at low temperature (<450 °C) (SnO, romarchite; Sn_3O_4; and SnO_2, cassiterite) and SnO (minor) and SnO_2 (major phase) at higher temperatures (>480 °C up to 500 °C). Constant temperature treatment at 500 °C results in sintered films; however, thermal oxidation at 500 °C after preheating at 200 °C produces films with good stability and with less sintering.

Spray-pyrolyzed tin oxide films consist of SnO_2 (cassiterite). Sn $M_4N_{45}N_{45}$ Auger transitions of tin and tin oxide materials show significant differences in peak shape, which are believed to be due to differences in oxidation states of Sn. The Auger peak intensity ratios of O $KL_{23}L_{23}$ to Sn $M_4N_{45}N_{45}$ can give information on the net oxidation state of Sn. Thin films made of SnO_2 (cassiterite) show lower sheet resistance than SnO (romarchite). The interfacial region between the thermally oxidized tin oxide layer and the substrate may be due to migration of tin oxides to the substrate or the substrate to the tin oxide layer or both. The O/Sn ratios of the films obtained by SAM and XPS are similar and less than 2, which means that the surfaces of the films are not consisted of pure SnO_2. Phase changes during thermal oxidation may explain increases in transmittance of these tin oxide films. Spray-coated tin oxide films with $SnCl_4$ have lower light absorbance in the UV−visible region than thermally oxidized films. Crystallinity of tin oxide films is more critical than surface morphology in gas sensing. Tin oxide films with mixed phases are better than single phase films for gas sensors. Tin oxides prepared by temperature-programmed thermal oxidation and spray pyrolysis showed reproducible responses that are related to the concentration of CH_2Cl_2.

Acknowledgment. We thank the State of Connecticut Department of Economic Development High Technology program, Connecticut Innovations, Inc., and Olin Corp. for support of this research.

CM970672X

(29) Park, S. H., Ph.D. Thesis, University of Connecticut, 1997.